IEEE Open Journal of
Antennas and Propagation

Received 25 January 2021; revised 11 April 2021; accepted 29 April 2021. Date of publication 10 May 2021; date of current version 18 May 2021.

Digital Object Identifier 10.1109/OJAP.2021.3078236

A Multifunctional Compact Pattern Reconfigurable Antenna With Four Radiation Patterns for Sub-GHz IoT Applications

SAEED A. HAYDHAH [1] (Student Member, IEEE), FABIEN FERRERO [2] (Member, IEEE), LEONARDO LIZZI [2] (Senior Member, IEEE), MOHAMMAD S. SHARAWI [3] (Senior Member, IEEE), AND AZZEDINE ZERGUINE [4] (Senior Member, IEEE)

[1]Electrical and Computer Engineering Department, Concordia University, Montréal, QC H3G 1S6, Canada

[2]Université Côte d'Azur, CNRS, LEAT, 06410 Sophia Antipolis, France

[3]Electrical Engineering Department, Polytechnique Montrél, Montréal, QC H3T 1J4, Canada

[4]Electrical Engineering Department, KFUPM, Dhahran 31261, Saudi Arabia

CORRESPONDING AUTHOR: S. A. HAYDHAH (e-mail: s_haydha@encs.concordia.ca)

This work was supported by the French Government, through the UCA JEDI Investments in the Future Project managed by the National Research Agency (ANR) with the reference number ANR-15-IDEX-0001.

ABSTRACT A compact pattern reconfigurable antenna with four radiation patterns is proposed for sub-GHz IoT applications. The antenna has two functional modes; Mode I has three uncorrelated patterns, while Mode II has electric and magnetic omnidirectional patterns. The resonant frequency of the antenna is 868 MHz with measured overlapped −6 dB impedance-bandwidths of 22 MHz and 20 MHz for Mode I and Mode II, respectively. The antenna is integrated in an 80×55 mm^2 terminal. The radiating elements consist of two meandered slots and one meandered monopole. Four pattern configurations are obtained with an average peak gain of 0 dBi, and an average radiation efficiency of 43.3%. Two of the patterns are with 5 dB directivity, and the other two are omnidirectional patterns. Pattern reconfigurability is achieved using four PIN diodes. The antenna is fabricated on a low-cost FR-4 substrate. By removing FR-4 material inside the slots, slots' radiation efficiencies were improved by 2.25 dB.

INDEX TERMS Reconfigurable antennas, IoT, pattern reconfigurable antenna, slot antennas, UHF.

I. INTRODUCTION

THE NUMBER of devices connected to the Internet is increasing rapidly [1]. These devices will be controlled or monitored wirelessly using the Internet of Things (IoT) technology. Hence, it is important to design antennas working for IoT applications to serve this huge number of connected devices to the network. Ultra High Frequencies (UHFs) are preferred for IoT applications because of their higher penetration in buildings and long distance coverage. Comparing IoT with mobile phone technology, the wireless link robustness must be enforced in IoT applications, as it may not be possible for the object to move to improve its network level connection. Thus, additional mechanisms should be integrated to compensate for channel multi-path and blockage effects. Diversity schemes can be used to improve average Signal to Noise ratio (SNR) and to improve the reliability of IoT wireless systems. Many solutions have been proposed in literature to achieve diversity with a compact antenna.

The use of slot radiators is a suitable approach to obtain more compact antenna systems. Over the years, many techniques to achieve pattern reconfigurable slot-based antennas have been proposed. In [2], a pattern reconfigurable square-ring patch antenna at 2 GHz with two different patterns is achieved. The antenna achieved a bandwidth of 50 MHz, good efficiencies and good gains, however, the resonant frequency is relatively high, only two patterns were achieved, single polarization is achieved, and the antenna size is large.

In [3], a pattern reconfigurable patch antenna with complementary split-ring resonators (CSRRs) on the ground plane at 2.4 GHz is proposed, and the slot is used in the ground plane to form the CSRRs providing patterns with 180° phase shift from the patch's pattern. This proposed antenna in [3] has nine different radiation patterns with gains around 5 dB and with good efficiencies. However, it uses 8 PIN diodes, the frequency of operation is relatively high, only one linear polarization is achieved, and the antenna size is bulky. In [4], a pattern reconfigurable antenna array with the use of slot antennas as the array elements at 2.4 GHz is achieved. The antenna has 10 different patterns with bandwidths of 100 MHz, gains around 1.5 dB, Envelope correlation coefficients (ECCs) below 0.5, and a compact size. However, the physical size of the antenna is large even though the used resonant frequency is 2.4 GHz, which is relatively high. In addition, ECCs between some of the pattern configurations in [4] are more than 0.5. In [5], a wide-band pattern reconfigurable tapered-slot antenna at 2 GHz is achieved, with four radiation patterns and 6 dB gains. However, the antenna size is very bulky and only four patterns with four PIN diodes are achieved. In [6], a pattern reconfigurable patch-slot-ring antenna at 2.4 GHz is achieved, and the slot is used to redirect the current paths on the patch and metallic structures. The antenna uses 6 PIN diodes for four pattern configurations, and the antenna size is very bulky. In [7], a pattern reconfigurable slot antenna at 5 GHz is achieved, and the slot is the main radiator, and two more slots are used such that anyone of them can be switched to work as a director or a reflector. The antenna has three different radiation patterns with wide bandwidths and good gains around 7.5 dB. However, the antenna has three layers; two of them are Rogers with very low loss, and the antenna size is bulky even thought the resonant frequency is relatively high. In [8], a compact pattern and polarization reconfigurable meandered monopole-based antenna is achieved by changing the monopoles' orientations. However, only two pattern configurations at relatively high frequency are achieved, and the achieved gains are −1 dB. On the other hand, the proposed antenna in this article achieved four different radiation patterns with good radiation gains, two linear polarizations and a very compact size at 868 MHz. The proposed antenna uses only four PIN diodes, and one lossy substrate FR4. In addition, ECCs between the used pattern configurations are always below 0.4, and the Monopole configuration achieved a gain of 1.6 dB.

In this paper, a multifunctional compact antenna system with reconfigurable pattern capabilities at 868 MHz is proposed. The pattern reconfigurability is achieved by reconfiguring the feeding network and by using the ground plane as a reflector. The antenna follows a credit card size to make it integrable in new IoT devices. In addition, the Envelope Correlation Coefficients (ECCs) between different patterns are minimized in order to maximize diversity. The novelty of the proposed antenna is shown in the achieved four different pattern configurations using four PIN diodes, obtained efficiencies for the configurations with the use of lossy and cheap FR-4 substrate, and in the achieved gains and ECC values between the four configurations even though the size of the proposed antenna is very small at the sub-GHz band. The size of the antenna follows a credit card size to make the antenna suitable for industrial applications; it is light and easy to be carried by workers for example. In addition, two functional modes are achieved by the proposed antenna; one mode is suitable for Line-of-sight applications, while the second mode is suitable for multipath environments. Furthermore, the proposed antenna achieved two orthogonal radiation patterns (electrical and magnetic omnidirectional patterns), and two very directive radiation patterns. These achievements are attained by the proposed antenna even though its size is relatively very small, and the RF-transceiver, the Arduino circuit and the battery are connected and attached directly to the antenna. The rest of the paper is organized as follows, Section II details the antenna geometry, Section III includes the simulation and measured results of the antenna, Section IV discusses some of the antenna results and compares the proposed antenna with previous antennas, and Section V concludes the paper.

II. ANTENNA GEOMETRY

A. ANTENNA ELEMENTS SELECTION

Many IoT applications require compactness to ease device integration in existing objects. Hence, a credit card form factor (80×50 mm^2) has been targeted for this proposed antenna. In this study, 3 radiating elements are integrated in the terminal, and a switching feeding circuit is used to select one of the three radiating elements. Different antenna designs, as shown in Fig. 1 and Fig. 2, were studied in order to determine the best antenna prototype. It is well-known that magnetic and electric dipoles provide orthogonal radiation patterns. On a compact surface, an electric dipole can be realized with a meandered line, while a magnetic dipole can be usually created with meandered slots.

During the early stages of the antenna design and as shown in Table 1, Fig. 1 and Fig. 2, many antenna designs were studied. It can be seen from Fig. 1(a) that the first antenna design included three slots at the antenna corners. Three pattern configurations were obtained. The patterns were omnidirectional along the xy-plane but directed more towards different corners for different configurations. The problem with this design was the high ECC values between slots located at the same edge as shown in Table 1 (ECC values above 0.8).

In the second design (as shown in Fig. 1(b)), two electric monopoles, positioned on the diagonal, were used to replace the two slots on the diagonal in an attempt to reduce the ECC values between the patterns. Unfortunately, the ECC values between the patterns of the two monopoles were also larger than 0.8 as shown in Table 1.

With two slots and one monopole as shown in Fig. 2, the best solution is obtained since the ECC values are well below

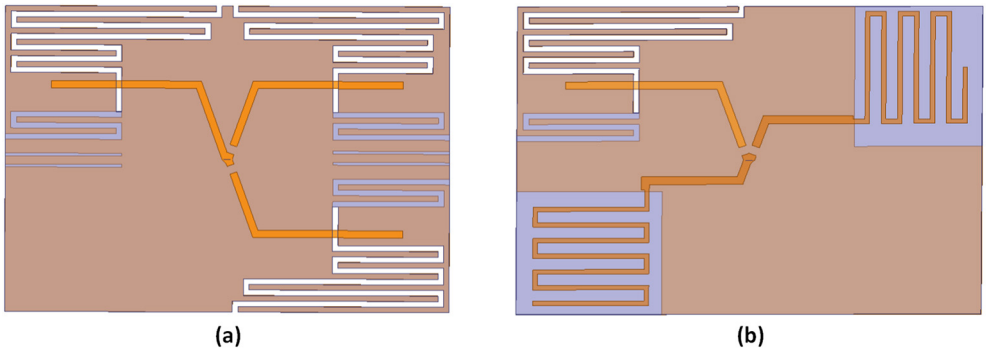

FIGURE 1. The attempted designs at the early stages of the proposed antenna. (a) The first antenna design. (b) The second antenna design.

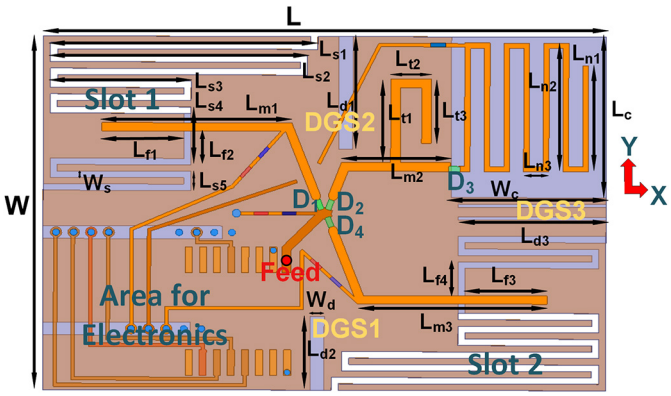

FIGURE 2. The geometry of the proposed antenna. Top face is in golden color, bottom face is in brown color, and substrate is in light blue color.

TABLE 1. Different antenna designs with preliminary ECC results.

Antenna Design	ECC, slots	ECC, mono.	ECC, slots&mono.
3 slots	> 0.8	-	-
1 slot,2 diag. mono.	-	> 0.8	< 0.5
2 diag. slots,1 mono.	< 0.1	-	< 0.4

diag. stands for diagonal, mono. sands for monopole.

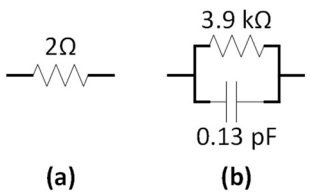

FIGURE 3. The used equivalent circuit models in the full-wave simulation for the different states of the PIN diode. (a) ON state PIN diode. (PIN diode is ON with 10 mA forward current). (b) OFF state PIN diode.

0.4 as shown in Table 1. This antenna provides four radiation patterns; i.e., two functional modes. Mode I has three uncorrelated patterns, and Mode II has electric and magnetic omnidirectional patterns. The ECC values between Slot 1 and Slot 2 configurations are low because the polarizations of the dominant electric fields of the two configurations are different. In addition, the two slots are not close to each others which helps in reducing the ECCs between the two configurations.

B. DESIGN DESCRIPTION

The proposed pattern reconfigurable antenna is designed on an FR-4 substrate with a dielectric constant of $\epsilon_r = 4.4$, a loss tangent of tan $\delta = 0.02$, and a thickness of $h = 0.8$ *mm*. The antenna geometry is shown in Fig. 2. The size of the antenna is 80×55 mm^2; i.e., the electrical size of the antenna is $0.23\lambda_0 \times 0.16\lambda_0$ at 868 MHz. It can be seen from Fig. 2 that the antenna is composed of one substrate with top and bottom faces. The top face includes the reconfigurable feeding network, the monopole and the biasing lines. The reconfigurable feeding network includes 50 Ω transmission lines and four PIN diodes (Infineon BAR64-02 V PIN diodes, 10 mA flow through the ON PIN diode, with a power consumption of 20 mW for the ON PIN diode); the PIN diodes are in green color in Fig. 2. The PIN diodes are used to control the feeding network. In addition, the equivalent circuit models for the different states of the used PIN diode are shown in Fig. 3; the equivalent circuit model for the ON state PIN diode is shown in Fig. 3(a), while the equivalent circuit model for the OFF state PIN diode is shown in Fig. 3(b). The equivalent circuit models for the different states of the PIN diode were used in the full-wave simulation during the simulations of the proposed antenna. The biasing networks for the PIN diodes, shown on the top face in Fig. 2, include RF chokes (in blue color) with 100 nH, and limiting resistors (in light red color) of 100 Ω to protect the diodes from overloading currents. Furthermore, the biasing lines have a width of 0.5 mm in order to enhance the isolation between the RF signals and the DC circuit. The bottom face of the antenna includes the ground plane (in brown color) where two meandered slots are etched, and a rectangular cut is etched also for the monopole to radiate. One feeding port is used for this design, and its position is shown in Fig. 2 with a red circle. The left-bottom corner of the terminal is available for electronic components used to control this reconfigurable antenna and to receive/transmit RF signals (i.e., an area for a microcontroller, a transceiver, and a small battery to operate these electronics).

This antenna is designed to operate at a resonant frequency of 868 MHz. Hence, the total length of each slot is 246 mm, and the monopole is meandered with a length of 142.87 mm.

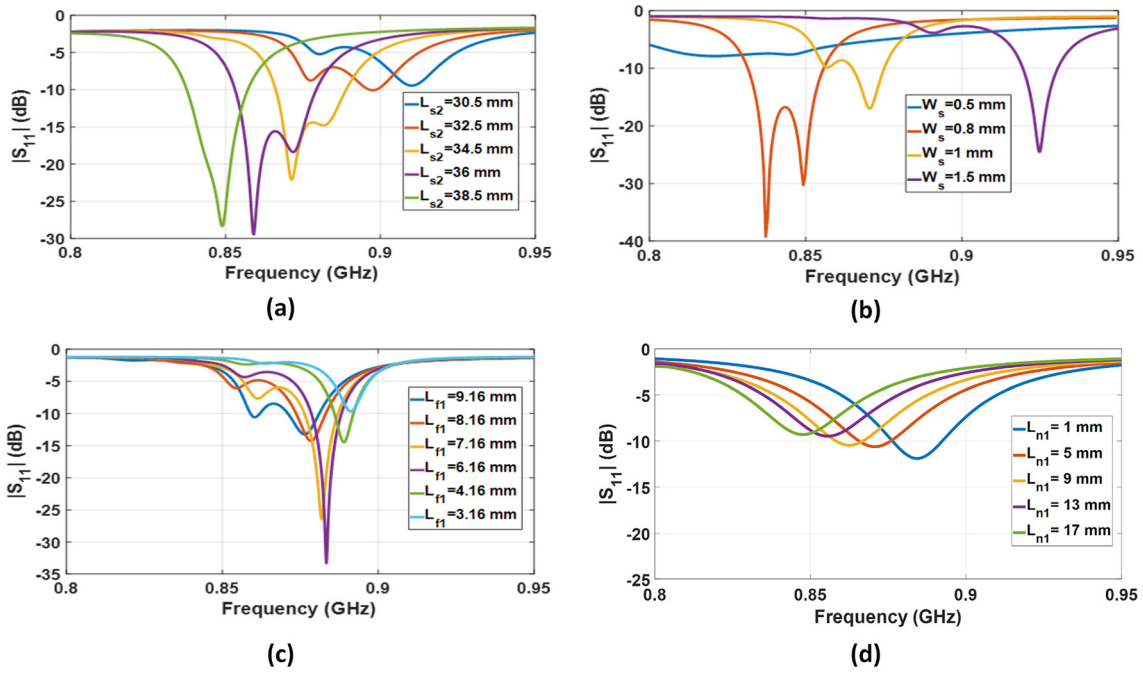

FIGURE 4. The simulated parametric analysis of the proposed pattern reconfigurable antenna. The scales are different for more clear view of the plots. (a) Parametric study on the length of slot (L_{s2}). (b) Parametric study on the slot-width (W_s). (c) Parametric study on the length of the feeding line after the slot (L_{f1}). (d) Parametric study on the length of the monopole (L_{n1}).

With reference to Fig. 2, the dimensions (in mm) of the antenna are reported in Table 2. The stub shown in Fig. 2 before the monopole is an open circuited stub designed to enhance the input impedance matching for the monopole configuration at 868 MHz. It can also be seen from Fig. 2 that there are many defected ground structures (DGS1, DGS2 and DGS3 in Fig. 2) in the ground plane used to reduce the current coupling between the monopole cut and the slots.

C. PARAMETRIC ANALYSIS

The antenna geometry has been optimized by analyzing the effects of the main geometrical parameters on the antenna resonant frequency and radiation characteristics. Fig. 4((a)–(d)) show the parametric studies on the length of slot L_{s2}, the width of the slot W_s, the length of the feeding line after the slot L_{f1}, and on the length of the monopole L_{n1}; these parameters are shown in Fig. 2. It can be seen from Fig. 4(a) that as the length of the slot increases, the resonant frequency of the antenna decreases. The used slot-width (W_s) for the proposed antenna is 1 mm, however, it can be seen from Fig. 4(b) that the resonant frequency is changed if the slot-width (W_s) was varied. In addition, it can be seen from Fig. 4(b) that as the slot-width decreases, the bandwidth of operation increases. Fig. 4(c) shows that the input impedance matching can be enhanced sharply if the parameter L_{f1} is properly optimized. In addition, the resonant frequency could vary if this parameter is varied. Finally, it can be seen from Fig. 4(d) that as the monopole length increases, the resonant frequency decreases.

D. RECONFIGURATION MECHANISM

This antenna provides four pattern configurations. The first pattern configuration, called Slot 1 configuration, is achieved when diode D1 only is ON. In this configuration, Slot 1 is radiating and the pattern is an omni-directional pattern of a magnetic dipole in the azimuthal plane, which is directed towards left-up corner because of the ground plane. The ground plane in this case is working as a reflector. The second pattern configuration, called the Monopole configuration, is achieved when both diodes D2 and D3 in Fig. 2 are ON, while the other diodes are OFF. In this configuration, the radiated pattern is an omni-directional pattern in the elevation plane. The third pattern configuration, called Slot 2 configuration, is achieved when the diode D4 only is ON. In this configuration, Slot 2 is radiating and the pattern is an omni-directional pattern in the azimuthal plane, and the pattern is directed towards the right-bottom corner. The fourth pattern configuration is achieved when Slot 1 and Slot 2 configurations are activated simultaneously. As a result, a pure magnetic omnidirectional pattern along the azimuthal plane is achieved.

Taking the ECC values shown in Table 3 into consideration, it can be seen that the proposed antenna has two functional modes. Mode I includes Slot 1 configuration, Slot 2 configuration, and the Monopole configuration because the ECC values between them is below 0.4. Hence, these three configurations of Mode I are uncorrelated. Mode II includes the Monopole configuration and the Slot 1&2 configuration because they are orthogonal to each

FIGURE 5. The fabricated pattern reconfigurable antenna with RF transceiver and battery on top face, and Arduino is on bottom face. (a) Top view. (b) Bottom view.

others. Hence, the two configurations of Mode II are also uncorrelated.

It is worth mentioning that the locations of the diodes D1, D2 and D4 in Fig. 2 are chosen such that the input impedance matching for all configurations is enhanced. Before adding the RF transceiver circuit to the antenna, the location of the feeding point was originally in the center between the diodes D1, D2 and D4, and the locations of these diodes were optimized such that best input impedance matching is achieved for the four pattern configurations. However, it is required to change the position of the feeding point off-center to the new point shown in Fig. 2 because this new point is the RF output of the RF transceiver. The impedance matching for the four configurations is still good even though the location of the feeding point has been changed; this is expected because the feeding point was moved between two points along a 50 Ω transmission line. In addition, it was noted that when Slot 1 or Slot 2 Configuration is activated, the monopole will radiate even though its diode D2 is switched OFF. The monopole radiates while its diode (D2) is OFF because the monopole is grounded. The diode D3 is used in order not to provide the ground for the monopole when its configuration is OFF. As a result, when Slot 1 or Slot 2 configuration is activated, the monopole diodes D2 and D3 are OFF, and the monopole will not radiate because it does not have a ground. Therefore, it can be seen from Fig. 2 that the Monopole configuration requires two diodes (D2 and D3), where D2 (when it is OFF) is used to maintain the impedance matching for Slot 1 configuration and Slot 2 configuration when they are activated, while D3 (when it is OFF) is used to avoid radiation from the monopole when Slot 1 configuration or Slot 2 configuration are activated. Hence, the use of diode D3 strongly reduces the ECCs between the patterns of the Monopole configuration and the Slots' configurations.

III. SIMULATED AND MEASURED RESULTS

The design was simulated in HFSS, and measured in a Satimo StarLAB after adding the circuit layout for the RF transceiver and the Arduino. The fabricated antenna is shown in Fig. 5.

The simulated and measured $|S_{11}|$ results for the four pattern configurations are shown in Fig. 6, where it can be seen that the resonant frequency is at 0.87 GHz for all the configurations. It can also be seen that the simulated −6 dB impedance bandwidths are 27 MHz, 27 MHz, 38 MHz, and 15 MHz for Slot 1, Slot 2, Monopole, and Slot 1&2 configurations, respectively. Therefore, the simulated overlapped −6 dB impedance bandwidths are 27 MHz and 15 MHz for Mode I and Mode II, respectively, which is enough for IoT applications. The measured overlapped −6 dB impedance bandwidths are 22 MHz and 20 MHz for Mode I and Mode II, respectively. The simulated peak gains for the four configurations are shown in Fig. 7(a), where it can be seen that the peak gains in the required bandwidth of operation are around 0.5 dB, 0.5 dB, 0.3 dB, and −3.75 dB for Slot 1, Slot 2, Monopole, and Slot 1&2 configurations, respectively. The measured peak gains are 0.5 dB, 1.4 dB, 1.58 dB, and −3.5 dB for Slot 1, Slot 2, Monopole, and Slot 1&2 configurations, respectively.

TABLE 2. Dimensions of the proposed antenna.

Parameter	Length (mm)	Parameter	Length (mm)
L	80	W	55
W_s	1	Monopole width	0.8
L_{s1}	38	L_{s2}	36.5
L_{s3}	20	L_{s4}	9
L_{s5}	3	L_{m1}	27
L_{m2}	15.5	L_{m3}	27
L_{f1}	11.66	L_{f2}	5.25
L_{f3}	11.66	L_{f4}	5.25
L_{n1}	16.5	L_{n2}	20
L_{n3}	3.6	L_{t1}	12.95
L_{t2}	5.76	L_{t3}	10
L_{d1}	17.5	L_{d2}	11.5
L_{d3}	21	L_c	25
W_c	22	W_d	1
h	0.8	Transmission line width	1.3

TABLE 3. Envelope correlation coefficients between the patterns of the antenna at 870 MHz.

Configuration	Slot 1	Monopole	Slot 2	Slot 1 and 2
Slot 1	1	0.26	0.03	0.57
Monopole	0.26	1	0.4	0.02
Slot 2	0.03	0.4	1	0.61
Slot 1 and 2	0.57	0.02	0.61	1

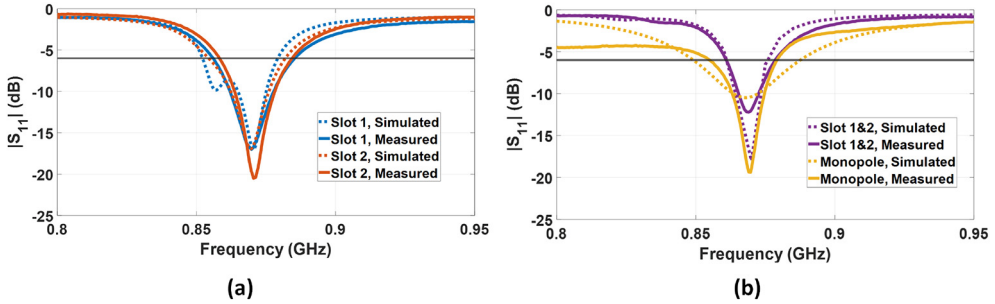

FIGURE 6. The simulated and measured $|S_{11}|$ results (in dB) of the proposed reconfigurable antenna. (a) Slot 1 and Slot 2 Configurations. (b) Slot 1&2 and Monopole Configurations.

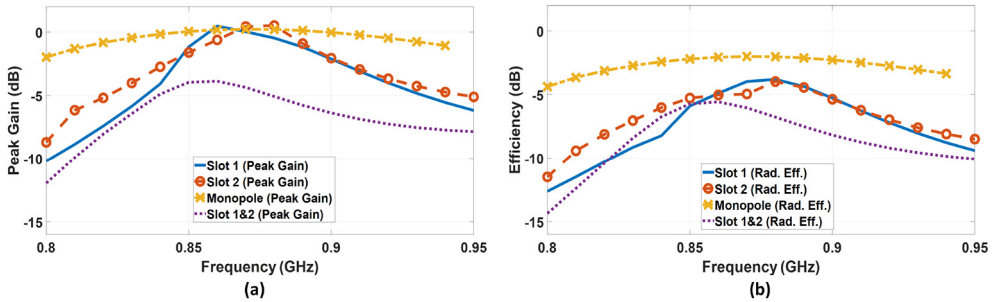

FIGURE 7. The simulated performance metrics (in dB) of the proposed reconfigurable antenna. (a) The peak gains of the four pattern configurations in dB. (b) The radiation efficiencies of the four pattern configurations in dB.

The simulated radiation efficiencies for the four configurations are shown in Fig. 7(b). The simulated efficiencies in the required bandwidth of operation are around 40%, 35%, 62%, and 28% for Slot 1, Slot 2, Monopole, and Slot 1&2 configurations, respectively, while the measured radiation efficiencies are about 36.8%, 40.5%, 70%, and 26% for Slot 1, Slot 2, Monopole, and Slot 1&2 configurations, respectively. These results are reasonable because the antenna is electrically small, and the used substrate is a lossy substrate. Hence, a degradation in the efficiencies and in the peak gains is expected. Nevertheless, the antenna still fulfills industrial requirements for IoT applications.

The simulated and measured 2D radiation patterns of the four configurations are shown in Fig. 8. The left-side pattern for each configuration shows the xy-plane cut, while the right-side pattern shows the pattern in the elevation plane at which the maximum peak gain is achieved. It can be seen from Figs. 8((a) and (b)) that the radiation pattern of Slot 1 configuration follows the radiation pattern of a magnetic dipole, but the pattern is directed towards $\phi = 145°$ because the ground plane works as a reflector. The simulated Half Power Beam Widths (HPBWs) are 130° and 110° in the azimuthal, and elevation planes, respectively. The measured HPBWs are 150° and 112° in the azimuthal, and elevation planes, respectively. The measured Front to Back Ratio (FTBR) is −15 dB. For Slot 2 Configuration, it can be seen from Figs. 8((c) and (d)) that the radiation pattern follows the pattern of a magnetic dipole, but the pattern is directed towards $\phi = -50°$. The simulated HPBWs are 110° and 120° in the azimuthal and elevation planes, respectively. The measured HPBWs are 114° and 115° in the azimuthal, and elevation planes, respectively. The measured FTBR is −8 dB. For the Monopole configuration, it can be seen from Fig. 8((e) and (f)) that the radiation pattern is an omnidirectional pattern along the elevation plane $\phi = 120°$ since the radiating element is an electrical monopole. The simulated HPBW is 85° in the azimuthal plane. The measured HPBW is 100° in the azimuthal plane. Finally, it can be seen from Fig. 8((g) and (h)) that the radiation pattern of the Slot 1&2 configuration is pure magnetic omnidirectional pattern along the azimuthal plane. The simulated HPBW is 100° in the elevation plane. The measured HPBW is 95° in the elevation plane.

In addition, it can be seen from Figs. 8((a), (c), (g), and (h)) that the differences between the co- and cross-polarization patterns for the slot configurations are above 20 dB. Hence, when one or both of the slots are radiating, the antenna radiates a pure horizontal polarization. For the monopole configuration on the other hand, it can be seen from Fig. 8(f) that the difference between co- and cross-polarization is around 5 dB at broadside and around it. Hence, this antenna radiates a vertical polarization as well when the Monopole configuration is activated. Therefore, this proposed antenna can also be considered as a polarization reconfigurable antenna. This polarization diversity enhances the receiving sensitivity of the antenna.

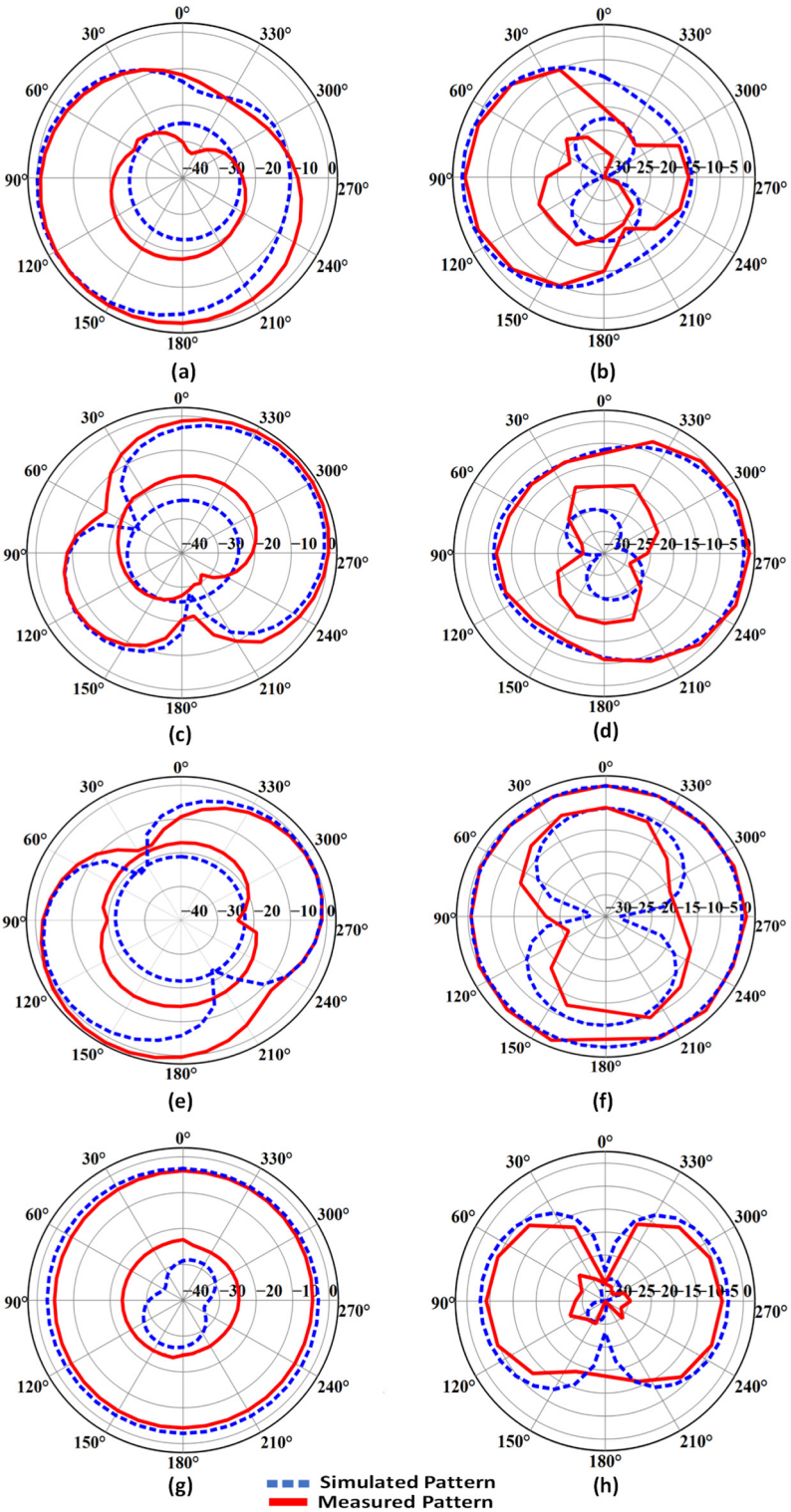

FIGURE 8. The simulated and measured 2D-patterns (in dB) of the proposed reconfigurable antenna for four configurations. (a) Slot 1 Configuration; x-y plane. (b) Slot 1 Configuration; Elevation plane. (c) Slot 2 Configuration; x-y plane. (d) Slot 2 Configuration; Elevation plane. (e) Monopole Configuration; x-y plane. (f) Monopole Configuration; Elevation plane. (g) Slot1&2 Configuration; x-y plane. (h) Slot1&2 Configuration; Elevation plane.

IV. DISCUSSIONS

It can be seen from Fig. 5 that some parts of the FR-4 substrate, where high electric field concentrations are available, are removed above Slot 1 and Slot 2 in order to enhance the radiation efficiencies (68% enhancement is achieved) as shown in Fig. 9. As a result, the slots' sides become flexible

TABLE 4. Comparison between the proposed antenna and some related references.

Ref.	$f_r(MHz)$	Avg. Eff. (%)	Electrical Size	Patterns num.	ECC	Max. Peak Gain (dB)	F.o.M.	APP.
[10]	750	57.3	$0.325\lambda_o \times 0.475\lambda_o$	4	<0.08	0	14.85	MIMO
[11]	850	45	$0.34\lambda_o \times 0.17\lambda_o$	2	<0.35	0	15.57	MIMO
[12]	850	50	$0.34\lambda_o \times 0.17\lambda_o$	2	<0.5	1	17.3	MIMO
[13]	775	65	$0.31\lambda_o \times 0.155\lambda_o$	2	<0.4	0	27.06	MIMO
[14]	2400	80	$0.31\lambda_o \times 0.57\lambda_o$	4	-	4	18.11	IoT
[15]	2400	-	$0.8\lambda_o \times 0.8\lambda_o$	8	-	5	12.5	WSN
[16]	2400	84	$0.5\lambda_o \times 0.5\lambda_o$	4	-	6	13.44	WSN
[17]	562	53.3	$0.49\lambda_o \times 0.49\lambda_o$	4	-	5	8.88	TV Signal Reception
This Work	868	49.1	$0.23\lambda_o \times 0.159\lambda_o$	3 (Mode I)	<0.4	1.6	40.28	IoT (Line-of-Sight Environment)
This Work	868	30	$0.23\lambda_o \times 0.159\lambda_o$	2 (Mode II)	<0.02	1.6	16.41	IoT (Multipath Environment)

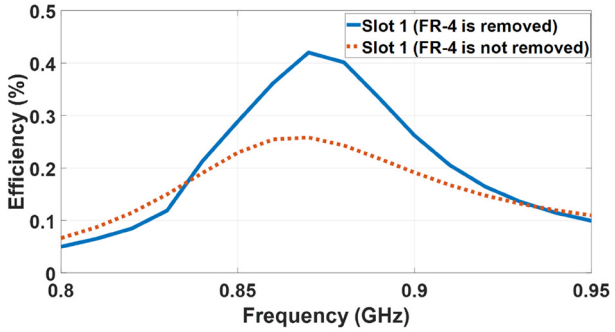

FIGURE 9. The efficiency variations due to the removal of FR-4 substrate behind parts of the radiating slots.

and robust. This antenna prototype has been realized through a commercially available process. Hence, this removal of some parts of FR-4 material did not add additional costs.

In addition, it is good to mention that the isolation between Slot 1 and Slot 2 was enhanced by 5 dB, thanks to the use of the Defected Ground Structures (DGS) in the ground plane. The isolation mentioned in the previous statement was found by applying three ports; one port for each radiating element, then the $|S_{21}|$ results were found between the three ports. At the bandwidth of operation, the obtained maximum simulated $|S_{21}|$ after adding DGS in the ground plane is $-$ 12.9 dB. Furthermore, the ECC values between the four patterns were calculated using the general field equation [4], [9]. The ECC values between the four patterns of this antenna at 0.87 GHz are shown in Table 3. The ECC values between the three pattern configurations of Mode I are well below 0.4; i.e., these patterns are uncorrelated. In addition, the ECC values between the pattern configurations of Mode II (Monopole and Slot 1&2 configurations) are 0.02 showing that these two patterns are almost orthogonal. It can be noticed that some performance metrics (e.g., ECC and isolation) of Multiple-Input Multiple-Output (MIMO) antennas are used for this work because this proposed antenna is a good candidate for MIMO applications if the bandwidth of operation is enhanced. This can be a future work for this antenna.

Furthermore, this proposed antenna is a multifunctional antenna where Mode I has two patterns with high directivity and one electric omnidirectional pattern, and Mode II has electric and magnetic omnidirectional patterns. Therefore, Mode I is suitable to be used in Line-of-Sight environments, where the multipath effects are negligible, such that the received SNR is enhanced by the use of the pattern reconfigurable Mode I of the proposed antenna. On the other hand, Mode II should be used in environments where the multipath effects are large because the use of uncorrelated omnidirectional patterns helps to enhance the received SNR in such environments.

Table 4 shows the comparison between the proposed antenna and some references available in the literature. References [10]–[13] are MIMO antennas for mobile terminals working at frequencies around 800 MHz. References [14]–[16] are pattern reconfigurable antennas for IoT applications but at a resonant frequency of 2.4 GHz, and [17] is a pattern reconfigurable antenna used for TV signal reception on moving vehicles and at a resonant frequency of 0.56 GHz. It can be seen that the proposed antenna has better results in terms of miniaturization, number of patterns, and achieved maximum peak gains when size and resonant frequencies are considered. It can also be seen that the proposed antenna has competing results with the previous works in terms of diversity and efficiency. A Figure of Merit (F.o.M.) equation was calculated using (1) to show that the proposed antenna has a better performance in terms of miniaturization, diversity and average efficiencies compared to previous works.

$$F.o.M. = \frac{Number\ of\ Patterns \times Avg.\ Efficiency}{Antenna\ Electrical\ Size} \quad (1)$$

The results of (1) are reported in Table 4 where it can be seen that the proposed antenna achieved better results among the other designs in terms of miniaturization, diversity and average efficiencies.

V. CONCLUSION

A new multifunctional compact pattern reconfigurable IoT antenna with two functional modes at 868 MHz is proposed; Mode I includes three uncorrelated patterns, and Mode II includes electric and magnetic omnidirectional patterns. The size of the antenna is a credit card size. The antenna is switched electrically. Four patterns are achieved by this antenna; two directional patterns and one electrical dipole pattern. The forth pattern is a pure magnetic omnidirectional

pattern achieved by combining the two directional patterns. The achieved pattern configurations of Mode I have efficiencies more than 37%, a measured overlapped −6 dB impedance bandwidth of 22 MHz, and ECCs which are well below 0.4. The achieved pattern configurations of Mode II have a measured overlapped −6 dB impedance bandwidth of 20 MHz, and the ECCs are 0.02. The achieved peak gains are above 0.5 dB when a single slot is radiating, and 1.6 dB for the Monopole configuration.

ACKNOWLEDGMENT

The authors would like to thank the CREMANT for its support.

REFERENCES

[1] "Cisco visual networking index: Global mobile data traffic forecast update, 2017–2022," Cisco, San Jose, CA, USA, White Paper, 2019. Accessed: Oct. 18, 2019. [Online]. Available: https://www.cisco.com/c/en/us/solutions/collateral/service-provider/visual-networking-index-vni/white-paper-c11-738429.html

[2] S.-H. Chen, J.-S. Row, and K.-L. Wong, "Reconfigurable square-ring patch antenna with pattern diversity," *IEEE Trans. Antennas Propag.*, vol. 55, no. 2, pp. 472–475, Feb. 2007.

[3] Z.-L. Lu, X.-X. Yang, and G.-N. Tan, "A multidirectional pattern-reconfigurable patch antenna with CSRR on the ground," *IEEE Antennas Wireless Propag. Lett.*, vol. 16, pp. 416–419, 2017.

[4] M.-L. Lai, T.-Y. Wu, J.-C. Hsieh, C.-H. Wang, and S.-K. Jeng, "Compact switched-beam antenna employing a four-element slot antenna array for digital home applications," *IEEE Trans. Antennas Propag.*, vol. 56, no. 9, pp. 2929–2936, Sep. 2008.

[5] Z.-L. Lu, X.-X. Yang, and G.-N. Tan, "A wideband printed tapered-slot antenna with pattern reconfigurability," *IEEE Antennas Wireless Propag. Lett.*, vol. 13, pp. 1613–1616, 2014.

[6] S. Nair and M. Ammann, "Reconfigurable antenna with elevation and azimuth beam switching," *IEEE Antennas Wireless Propag. Lett.*, vol. 9, pp. 367–370, 2010.

[7] Y. F. Cao and X. Y. Zhang, "A wideband beam-steerable slot antenna using artificial magnetic conductors with simple structure," *IEEE Trans. Antennas Propag.*, vol. 66, no. 4, pp. 1685–1694, Apr. 2018.

[8] S. Raman, P. Mohanan, N. Timmons, and J. Morrison, "Microstrip-fed pattern- and polarization- reconfigurable compact truncated monopole antenna," *IEEE Antennas Wireless Propag. Lett.*, vol. 12, pp. 710–713, 2013.

[9] M. S. Sharawi, "Printed multi-band MIMO antenna systems and their performance metrics [wireless corner]," *IEEE Antennas Propag. Mag.*, vol. 55, no. 5, pp. 218–232, Oct. 2013.

[10] L. H. Trinh, F. Ferrero, L. Lizzi, J.-M. Ribero, and R. Staraj, "4×4 MIMO multiband antenna system for mobile handsets," *Int. J. Antennas Propag.*, vol. 2015, pp. 1–6, Dec. 2015.

[11] A. Cihangir, F. Ferrero, G. Jacquemod, P. Brachat, and C. Luxey, "Neutralized coupling elements for MIMO operation in 4G mobile terminals," *IEEE Antennas Wireless Propag. Lett.*, vol. 13, pp. 141–144, 2014.

[12] S. Zhang, K. Zhao, Z. Ying, and S. He, "Diagonal antenna-chassis mode for wideband LTE MIMO antenna arrays in mobile handsets," in *Proc. Int. Workshop Antenna Technol. (IWAT)*, Karlsruhe, Germany, 2013, pp. 407–410.

[13] S. Zhang, A. A. Glazunov, Z. Ying, and S. He, "Reduction of the envelope correlation coefficient with improved total efficiency for mobile LTE MIMO antenna arrays: Mutual scattering mode," *IEEE Trans. Antennas Propag.*, vol. 61, no. 6, pp. 3280–3291, Jun. 2013.

[14] L. H. Trinh, T. N. Le, R. Staraj, F. Ferrero, and L. Lizzi, "A pattern-reconfigurable slot antenna for IoT network concentrators," *Electronics*, vol. 6, no. 4, p. 105, 2017, doi: 10.3390/electronics6040105.

[15] L. Catarinucci, S. Guglielmi, R. Colella, and L. Tarricone, "Compact switched-beam antennas enabling novel power-efficient wireless sensor networks," *IEEE Sensors J.*, vol. 14, no. 9, pp. 3252–3259, Sep. 2014, doi: 10.1109/jsen.2014.2326971.

[16] T. N. Le, A. Pegatoquet, T. Le Huy, L. Lizzi, and F. Ferrero, "Improving energy efficiency of mobile WSN using reconfigurable directional antennas," *IEEE Commun. Lett.*, vol. 20, no. 6, pp. 1243–1246, Jun. 2016, doi: 10.1109/lcomm.2016.2554544.

[17] C. Kittiyanpunya and M. Krairiksh, "A four-beam pattern reconfigurable Yagi-Uda antenna," *IEEE Trans. Antennas Propag.*, vol. 61, no. 12, pp. 6210–6214, Dec. 2013, doi: 10.1109/tap.2013.2282914.

SAEED A. HAYDHAH (Student Member, IEEE) received the M.Sc. degree from the King Fahd University of Petroleum and Minerals, Dhahran, Saudi Arabia, in 2019. He is currently pursuing the Ph.D. degree in the field of antennas/radio frequency engineering with the Electrical and Computer Department, Concordia University, Montréal, QC, Canada. From 2019 to 2020, he was a visiting student with the Laboratory of Electronics, Antennas and Telecommunications, Université Côte d'Azur, Sophia Antipolis, France. During his M.Sc., he was a member of Antennas and Microwave Structure Design Laboratory, KFUPM.

FABIEN FERRERO (Member, IEEE) received the Ph.D. degree in electrical engineering from the University of Nice-Sophia Antipolis in 2007. From 2008 to 2009, he worked for IMRA Europe (Aisin Seiki Research Center) as a Research Engineer and developed automotive antennas. In 2010, he is recruited as an Associate Professor with the Polytechnic School,Université Nice Sophia-Antipolis. Since 2018, he has been a Full Professor with the Université Côte d'Azur. His studies concerned the design and measurement of millimetric antennas, IoT systems, and reconfigurable antennas. He is a member of LEAT (Laboratoire d'Electronique, Antennes et Telecommunications).

LEONARDO LIZZI (Senior Member, IEEE) received the M.Sc. degree in telecommunication engineering and the Ph.D. degree in information and communication technology from the University of Trento, Italy, in 2007 and 2011, respectively. During his Ph.D., he has been a Visiting Researcher with the Pennsylvania State University, USA, and the University of Nagasaki, Japan. From 2011 to 2014, he was a Postdoctoral Researcher with the Laboratory of Electronics, Antennas and Telecommunications, Université Côte d'Azur, Sophia Antipolis, France, where he has been a Maître de Conférences (an Associated Professor) Since 2014. At the moment, his research focuses on reconfigurable, miniature, multistandards antennas for Internet-of-Things applications, wearable devices, and 5G terminals.

MOHAMMAD S. SHARAWI (Senior Member, IEEE) is a Professor of Electrical Engineering with Polytechnique Montréal, Montréal, QC, Canada, where he is also a member of the Poly-Grames Research Center. He was with the King Fahd University of Petroleum and Minerals (KFUPM), Saudi Arabia, from 2009 to 2018. He founded and directed the Antennas and Microwave Structure Design Laboratory, KFUPM. He was a Visiting Professor with the Intelligent Radio (iRadio) Laboratory, Electrical Engineering Department, University of Calgary, Alberta, Canada, during the Summer-Fall of 2014. He was a Visiting Research Professor with Oakland University during the summer of 2013. He has more than 300 papers published in refereed journals and international conferences, ten book chapters, one single authored book entitled *Printed MIMO Antenna Engineering* (Artech House, 2014), and the lead authored the recent book *Design and Applications of Active Integrated Antennas* (Artech House, 2018). He has 25 issued and 12 pending patents in the U.S. Patent Office. His areas of research include multiband printed multiple-input-multiple-output (MIMO) antenna systems, reconfigurable and active integrated antennas, applied electromagnetics, millimeter-wave MIMO antennas, and integrated 4G/5G antennas for wireless handsets and access points.

Prof. Sharawi is serving as the Associate Editor for the IEEE ANTENNAS AND WIRELESS PROPAGATION LETTERS, *IET Microwaves, Antennas and Propagation*, and an Area Editor for *Microwave and Optical Technology Letters* (Wiley). He is the Specialty Editor of the newly launched *Frontiers in Communications and Networks Journal*-the System and Test-Bed Design section. He served on the Technical and organizational program committees of several international conferences, such as EuCAP, APS, IMWS-5G, APCAP, iWAT, and among many others.

AZZEDINE ZERGUINE (Senior Member, IEEE) received the B.Sc. degree in electrical engineering from Case Western Reserve University, Cleveland, OH, USA, in 1981, the M.Sc. degree in electrical engineering degree from the King Fahd University of Petroleum and Minerals (KFUPM), Dhahran, Saudi Arabia, in 1990, and the Ph.D. degree in electrical engineering from Loughborough University, Loughborough, U.K., in 1996. He is a Professor with the Department of Electrical Engineering, KFUPM. His research interests include signal processing for wireless communications, adaptive filtering, neural networks, and blind source separation an equalization. He was a recipient of the Three Best Teaching Awards at KFUPM, in 2000, 2005, and 2011, and the Best Research Award at KFUPM, in 2017. He is serving as an Associate Editor for the *IET Signal Processing* and the *EURASIP Journal on Advances in Signal Processing*.